Soils and Foundations 2013;53(5):756–773

The Japanese Geotechnical Society

Soils and Foundations

www.sciencedirect.com
journal homepage: www.elsevier.com/locate/sandf

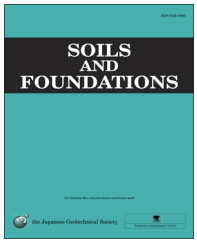

Finite element analysis of a deep excavation: A case study from the Bangkok MRT

Suched Likitlersuang[a,*], Chanaton Surarak[b,d], Dariusz Wanatowski[c], Erwin Oh[d], Arumugam Balasubramaniam[d]

[a]Department of Civil Engineering, Faculty of Engineering, Chulalongkorn University, Bangkok, Thailand
[b]Command and General Staff College, Royal Thai Army, Thailand
[c]Faculty of Science and Engineering, University of Nottingham Ningbo, China
[d]School of Engineering, Griffith University, Gold Coast Campus, Queensland, Australia

Received 9 November 2012; received in revised form 26 June 2013; accepted 24 July 2013
Available online 24 September 2013

Abstract

The Bangkok metropolitan area, located on a thick river soft clay deposit, has recently started a construction project on a mass rapid transit underground railway (MRT). This paper presents a finite element study on the Bangkok MRT underground construction project. The excavation of Sukhumvit Station was selected as the case study for the FEM numerical modelling in this paper. The numerical study focuses on the initial input on the ground conditions and the constitutive soil models. The geotechnical parameters were selected based on the soil investigation reports carried out for the purpose of the construction. The parameters selected for the constitutive models used in the FEM analysis were calibrated against the laboratory testing results. Finally, all the FEM simulations were compared with the data from field investigations.

Keywords: Deep excavation; Finite element method; Mass rapid transit; Bangkok clay

1. Introduction

Geotechnical design and construction on/in soft to very soft soils are usually associated with substantial difficulties. Since these types of soils are sensitive to deformations and possess low shear strength, their use may lead to structural damage during construction as well as throughout the life of the projects. This can come from (i) excessive settlements or the tilting of the newly constructed building structures, (ii) entrainment settlements of old structures near the newly erected structures and/or (iii) the adverse effect of excavations on nearby structures (Kempfert and Gebreselassie, 2006).

In Thailand, there is a large river deposit in the Central Plain region called the Chao Praya Delta. It is well-known that the delta consists of a broad basin filled with sedimentary soils, especially a thick soft to very soft clay layer deposited on the top. Importantly, the Bangkok metropolis – one of the largest commercial cities in South-East Asia – is also located on the low flat Chao Praya Delta in the Central Plain region of Thailand. There have been several construction projects to improve the quality of the infrastructure over the past 50 years.

*Corresponding author.
E-mail addresses: suched.l@eng.chula.ac.th (S. Likitlersuang), chanatons@gmail.com (C. Surarak), d.wanatowski@nottingham.edu.cn (D. Wanatowski), e.oh@griffith.edu.au (E. Oh), a.bala@griffith.edu.au (A. Balasubramaniam).

Peer review under responsibility of The Japanese Geotechnical Society.

Production and hosting by Elsevier

0038-0806
http://dx.doi.org/10.1016/j.sandf.2013.08.013

One of the most recent mega construction projects in Bangkok is the Bangkok Mass Rapid Transit (MRT) Underground Railway. This project involves significant geotechnical works, particularly foundations and excavations.

Nowadays, some commercial FEM codes, written especially for geotechnical problems, are used to analyse stability and ground movement due to excavations. Various constitutive soil models, from a simple elastic model to mathematically complex non-linear elasto-plastic models, have been developed to explain the strength and the deformation behaviour of soft soils. However, there is still a problem with predicting the movements in and around an excavation using numerical methods. The results of a numerical analysis may be influenced by many factors, such as simplified geometry and boundary conditions, mesh generation, the initial input of the ground conditions and the constitutive relationship chosen to model the behaviour of the soils. An example of a recent finite element study is the analysis of the behaviour of a mechanically stabilized earth wall (Bourgeois et al., 2012).

This paper aims to present a simplified two-dimensional finite element study of a deep excavation in soft clays. The FEM code, PLAXIS, is selected as the numerical tool and the Bangkok MRT underground construction project is chosen as the case study. The analysis focuses on the initial input of the ground conditions and the constitutive soil models. All the FEM simulations are compared with the data from field investigations.

1.1. Bangkok MRT project

The first phase of the Bangkok Metropolitan Rapid Transit (MRT) Underground Railway, named the Chaloem Ratchamongkhon (or the Blue Line), runs between Hua Lamphong and Bang Sue; it was completed in 2004. It comprises approximately 20 km of tunnels, constructed with tunnel boring machines (TBM). The route of the MRT Blue Line project is presented in Fig. 1. The project was constructed along highly congested roads in the heart of Bangkok City. The tunnel alignment, which is 22 km in length, includes 18 cut-and-cover underground stations, and is divided into two major sections, i.e., North and South (see Fig. 1 (a) and refer to Table 1). The underground stations are typically composed of three levels of structure, namely, the Centre Platform, the Side Platform and the Stacked Platform, as shown in Fig. 1(b). The stations are up to 230 m long and approximately 25 m wide, and are excavated up to a depth of 16–32 m below the ground surface. The station perimeter was constructed of diaphragm walls (D-walls), 1.0–1.2 m thick and 20–46 m deep. The tunnel lining consists of twin bored single-track tunnels. Each tube has a concrete segmental lining with an outer diameter of 6.3 m and an inner diameter of 5.7 m.

A total of 18 underground stations were constructed using the Top-Down construction technique, together with diaphragm walls (D-walls) and concrete slabs as excavation supports. A total tunnel length of 20 km was created using eight Earth Pressure Balance (EPB) shields. The excavation depths and D-wall lengths are plotted in Fig. 2. The stacked platform stations (S2, S3 and S4) had greater excavation depths and D-wall lengths than the centre and side-by-side platform stations. The majority of the centre and side-by-side platform stations (except stations S1 and N9) had similar excavation depths (about 21–22 m). However, the embedded depth of the D-walls differed between the North and South contracts due to the different design criteria (Phienwej, 2008). More details on the construction methods for tunnels and underground stations of the existing MRT Blue Line project can be found in Suwansawat (2002) and Suwansawat et al. (2007).

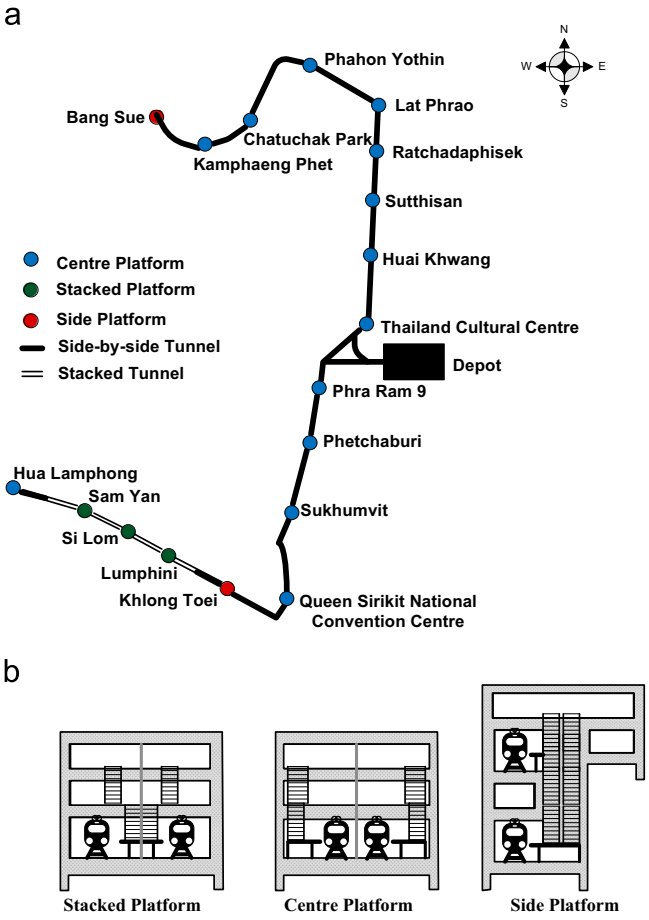

Fig. 1. Bangkok MRT Blue Line project. (a) Bangkok MRT Blue Line route. (b) Types of underground stations.

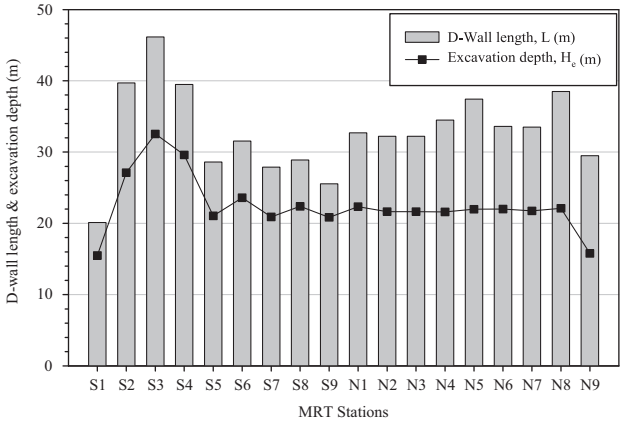

Fig. 2. Excavation depths and D-wall lengths of Bangkok MRT Blue Line stations (after Phienwej 2008).

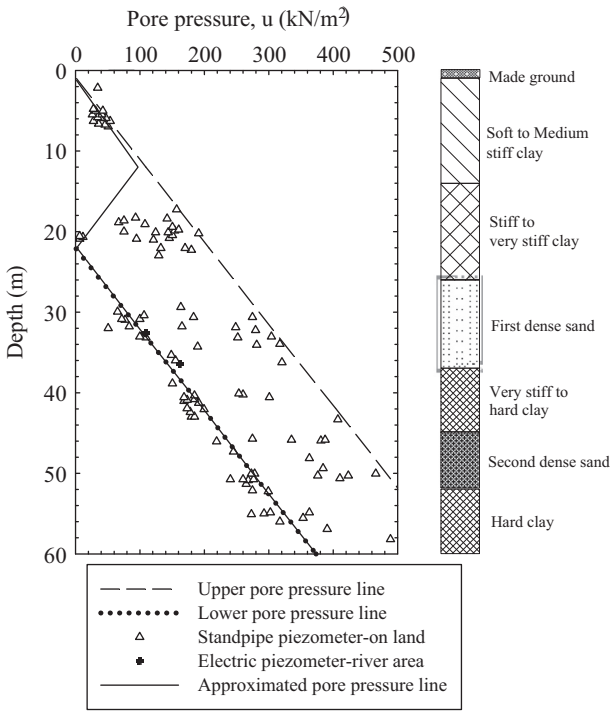

Fig. 3. Pore pressure in Bangkok subsoils.

1.2. Geological conditions of the central plain of Thailand

Bangkok subsoil forms a part of the larger Chao Phraya Plain and consists of a broad basin filled with sedimentary soil deposits. These deposits form alternate layers of sand, and clay. Field exploration and laboratory tests from the MRT Blue Line project show that the subsoils, down to a maximum drilling depth of approximately 60–65 m, can be roughly divided into (1) Made Ground at 0–1 m, (2) Soft to Medium Stiff Clays at 1–14 m, (3) Stiff to Very Stiff Clays at 14–26 m, (4) First Dense Sand at 26–37 m, (5) Very Stiff to Hard Clays at 37–45 m, (6) Second Dense Sand at 45–52 m and then (7) Very Stiff to Hard Clays (see Figs. 3 and 7). The aquifer system beneath the city area is very complex and the deep well pumping from the aquifers, over the last 50 years, has caused substantial piezometric drawdown in the upper soft and highly compressible clay layers, as presented in Fig. 3.

2. Retaining wall movements and ground settlements induced by excavations

2.1. Models for retaining wall displacements and ground settlements

The patterns of the retaining wall movements are governed by many factors, such as the type of subsoil encountered, the support system of the retaining wall (i.e., braced or anchored), the quality of the workmanship. Ou (2006) categorised the types of wall movements as cantilever or deep inward (or braced) excavations, as illustrated in Fig. 4. At the initial stage of excavation, or when the encountered soil is predominantly sandy, a cantilever type of movement tends to occur. As the

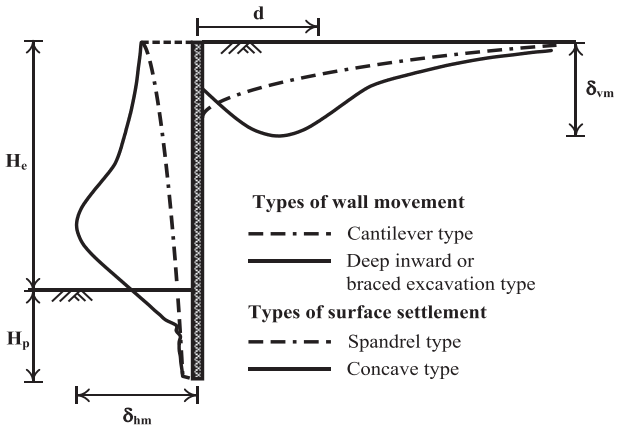

Fig. 4. Types of wall movement and ground surface settlement (after Hsieh and Ou, 1998; Ou, 2006).

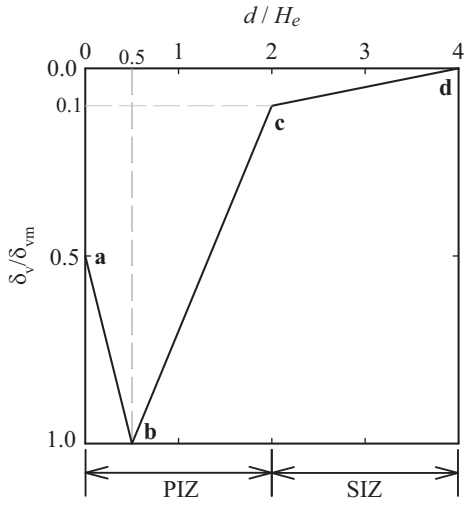

Fig. 5. Estimation of ground concave surface settlement (after Hsieh and Ou, 1998).

excavation proceeds further, especially in soft soils, a deep inward movement is more likely to be encountered.

Furthermore, the ground surface settlements induced by the excavations can be divided into two groups. According to Hsieh and Ou (1998), these are (i) the spandrel type, in which the maximum surface settlement is located near the wall and (ii) the concave type, in which the maximum surface settlement occurs at a distance away from the wall. Ou (2006) suggested that the spandrel surface settlement profile is likely to occur with the cantilever pattern of wall movements, while the concave surface settlement profile is likely to occur with the deep inward movement pattern.

2.2. Empirical predictions for excavation-induced ground movements

The first empirically based method to predict ground settlements, induced by excavations, was proposed by Peck (1969). Using a monitoring database of many case histories, Peck established a relationship between ground surface settlements,

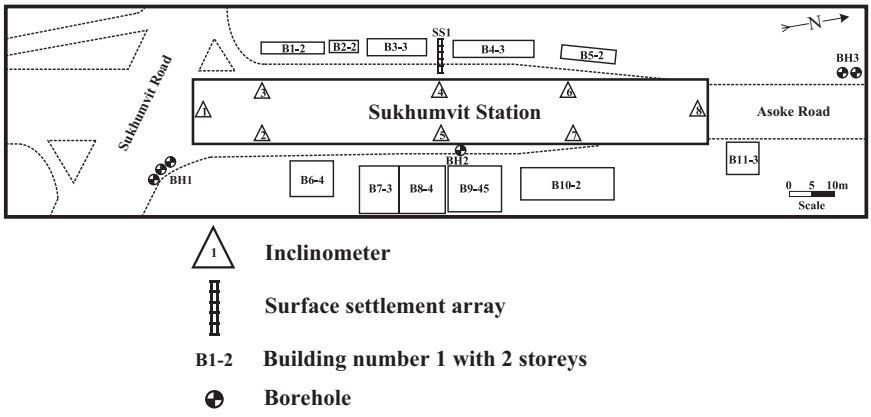

Fig. 6. Plan view of Sukhumvit Station and its instrumentations.

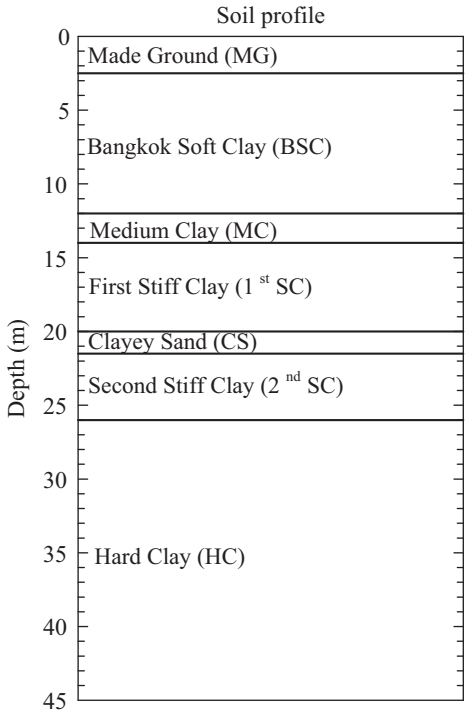

Fig. 7. Soil profile at the Sukhumvit Station location.

soil types, excavated depths and workmanship quality. The monitoring data were obtained mainly from steel sheet piles or soldier piles; these piles are quite different from those used in more recent construction methods (i.e., diaphragm walls with braced or anchored supports). Indeed, Ou (2006) stated that Peck's method may not necessarily be applicable to all excavation types. Similar to Peck's (1969) method, Clough and O'Rourke (1990) proposed a more refined set of surface settlement envelopes induced by an excavation. The shape and magnitude of the surface settlement envelopes depend on the type of soil, the excavation depth (H_e) and the maximum wall deflection (δ_{hm}).

Hsieh and Ou (1998) further refined Clough and O'Rourke's (1990) method by introducing two zones of influence, namely, the Primary Influence Zone (PIZ) and the Secondary Influence Zone (SIZ). The depth of the excavation (H_e) was set as the normalised parameter to predict the length of each zone. The concave settlement profile was proposed as the bi-linear relationship shown in Fig. 5. The surface settlements in the PIZ and SIZ are predicted using Eqs. (1) and (2), respectively:

$$\delta_v = \left(-0.636\sqrt{\frac{d}{H_e}}+1\right)\delta_{vm}, \quad \text{if } d/H_e \le 2 \quad \text{and} \tag{1}$$

$$\delta_v = \left(-0.171\sqrt{\frac{d}{H_e}}+0.342\right)\delta_{vm}, \quad \text{if } 2 \le d/H_e \le 4 \tag{2}$$

where δ_v and δ_{vm} are the surface settlement and the maximum surface settlement, respectively, of the soil at distance d from the wall. To continue the earlier work of Hsieh and Ou (1998), Ou and Hsieh (2011) suggested new surface settlement patterns, which take into account not only the excavation depth, but also the excavation width and the depth to the hard stratum.

Unlike Peck (1969) and Clough and O'Rourke (1990), in whose studies the shapes of the surface settlements are distinguished primarily by soil types, Hsieh and Ou (1998) and Ou and Hsieh (2011) classified the shapes of the surface settlements as spandrel or concave, as presented earlier in Fig. 4.

3. Bangkok MRT case study: Sukhumvit Station

Sukhumvit Station, located underneath Asok Road, next to the Sukhumvit – Asok intersection, as shown in Fig. 6, was selected for this study. The station box is located in a congested area surrounded by many commercial (3–4 stories) and residential buildings. Sukhumvit Station is also a connecting station between the MRT underground system and the Bangkok Mass Transit System (BTS) – an elevated train system at Asok Station. The soil profile consists of 2–3 m of Made Ground (MG), underlain by approximately 9 m of normally consolidated Bangkok Soft Clay (BSC), with an undrained shear strength of about 20 kN/m^2. The undrained shear strength of this layer tends to increase with depth from the level below 7 m. Beneath the BSC layer, there are 2 m of Medium Clay (MC), with an undrained shear strength of more

Table 1
Summary of MRT station dimensions, excavation depths and D-wall lengths.

Notation	Station	Station dimensions		Excavation depth, H_e (m)	D-wall length, L (m)
		Length (m)	Width (m)		
S1	Hua Lamphong	211	22	15.5	20.1
S2	Sam Yan	178	20	27.1	39.7
S3	Si Lom	154	28	32.6	46.2
S4	Lumphini	230	25	29.6	39.5
S5	Khlong Toei	230	25	21.1	28.6
S6	Queen Sirikit National Convention Center	230	25	23.6	31.6
S7	Sukhumvit	200	23	20.9	27.9
S8	Phetcaburi	199	23	22.4	28.9
S9	Phra Ram 9	400	26	20.9	25.6
N1	Thailand Cultural Centre	358	29	22.4	32.7
N2	Huai Khwang	228	25	21.7	32.2
N3	Sutthisan	228	25	21.7	32.2
N4	Ratchadaphisek	228	25	21.6	34.5
N5	Lad Phrao	293	25	22.0	37.4
N6	Phahon Yothin	228	25	22.0	33.6
N7	Chatuchak Park	364	32	21.8	33.5
N8	Kamphaeng Phet	228	25	22.1	38.5
N9	Bang Sue	228	32	15.8	29.5

than 60 kN/m^2. A thin, but continuous, medium dense Clayey Sand (CS) of 1.5 m is sandwiched between the First and Second Stiff Clays (1st SC and 2nd SC), with thicknesses of 6 m and 4 m, respectively. At a depth of 23–40 m, the Hard Clay (HC) layer (SPT N values of 30–40), with some sand lenses, is found. This HC layer is then underlain by the Dense Sand (DS) layer, up to 60 m deep. The ground water level at this location was found at 1.5 m below the ground surface. A schematic diagram of the Sukhumvit Station soil profile is shown in Fig. 7. It is noted that this soil profile was simplified based on a site investigation programme consisting of a series of four boreholes (Fig. 6).

3.1. MRT underground station construction

Sukhumvit Station was constructed using the Top-Down construction method, with a configuration of the centre platform type. The station box had a width, length and depth of 23 × 200 × 21 m. The reinforced concrete diaphragm walls (D-walls) were 1 m thick and 27.9 m deep; they were used for earth-retaining and permanent structures in the station. The concrete slabs of the first, second and third levels (Roof, Access and Concourse levels) were 1 m thick and the base slab was 1.8 m thick; these slabs were the primary braced support system for the D-walls. Figs. 6 and 8 show the plan view and the cross section geometry of Sukhumvit Station, respectively. The construction sequences adopted in the station box construction simulation are summarised in Table 2.

3.2. Monitoring system

Extensive instrumentation programs were adopted to monitor the deflection of the diaphragm walls and the ground settlements induced by the deep excavations. The instrumentation included

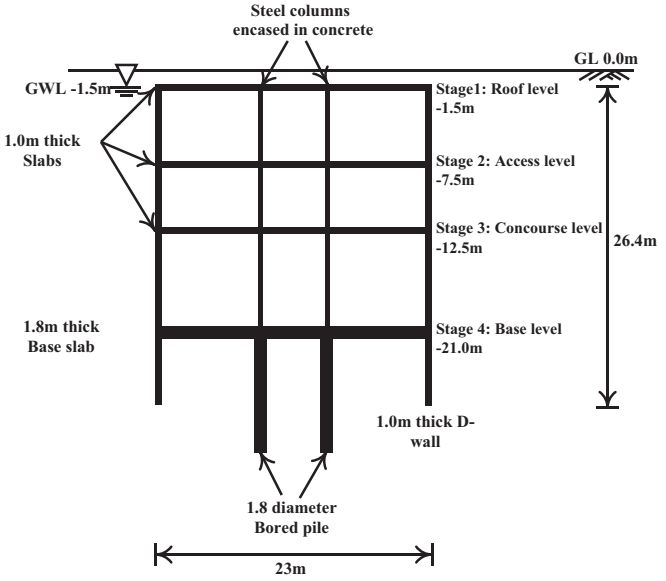

Fig. 8. Geometry of Sukhumvit Station.

inclinometers installed in the D-walls, inclinometers combined with extensometers, surface settlement points and surface settlement arrays. Building settlement points, tilt metres and crack metres were also installed to ensure that any damage to adjacent buildings would be kept within the design limitations. All instruments and adjacent borehole locations are depicted in Fig. 6. These instruments are composed of eight sets of inclinometers installed in the D-walls at various locations and one set of surface settlement arrays (SS1). The surface settlement (SS1) selection of this location was chosen because the surface settlement arrays (SS1) were located in a bare area between buildings B3 and B4. Thus, the surface settlement measured from SS1 could be considered as close to a greenfield condition. Moreover, the location of SS1 was in the middle of

Table 2
Construction sequences of Sukhumvit Station.

Sequences	Construction activities
1	Construction of diaphragm walls
2	Construction of bored piles
3	Installation of steel columns, which were plunged into the top of bored piles to form pin piles
4	Pre-excavation and placement of temporary steel decking supported by pin piles for traffic diversion
5	Excavation to level of underside of temporary prop and installation of temporary prop
6	Excavation to level of underside of roof slab and construction of permanent concrete roof slab
7	Removal of temporary prop
8	Excavation to level of underside of second slab level
9	Construction of second concrete slab
10	Stages 8 and 9 were repeated for third and fourth (base) slabs
11	Composite columns were installed
12	Backfill roof slab and final road reinstatement

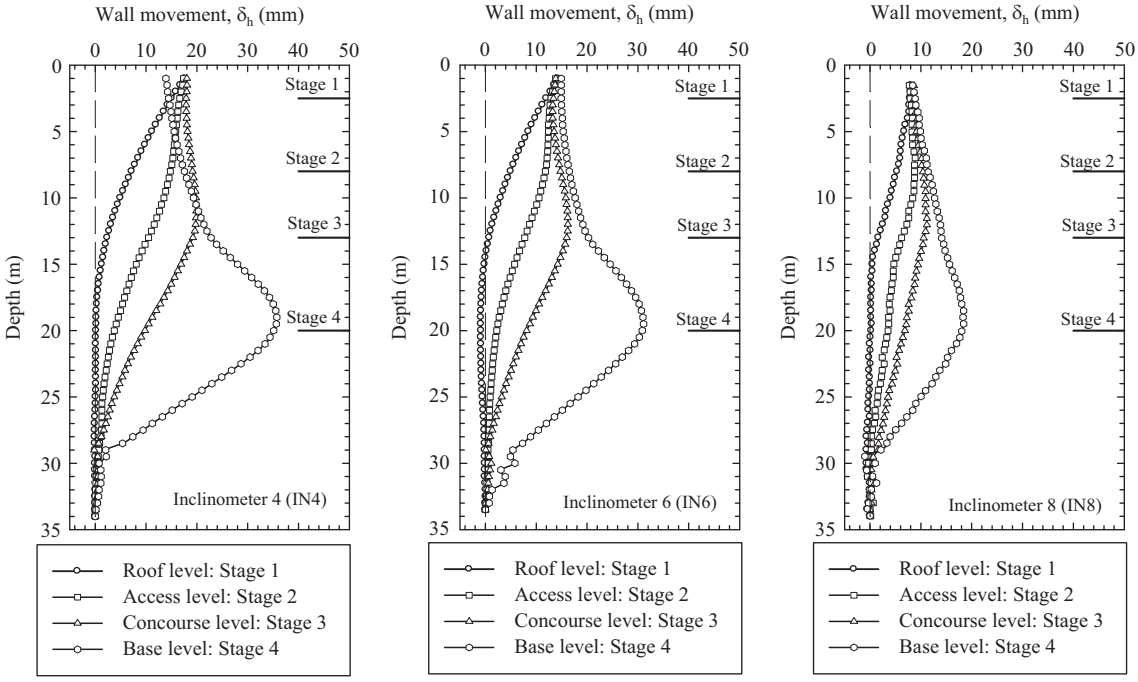

Fig. 9. Horizontal movement of diaphragm walls from inclinometers 4, 6 and 8.

the North–South length of Sukhumvit Station, where the effects of the corners were expected to be minimised. For this reason, inclinometer number 4 (IN4) will also be used in the present study to verify the two-dimensional finite element analysis.

3.3. Diaphragm wall movements

The field observations from the inclinometers revealed that the cantilever pattern developed after the first excavation stage. As the excavation proceeded to a greater depth, the D-walls showed braced excavation patterns with a bulge in the first stiff clay layer. Fig. 9 shows the four stages of the diaphragm wall movements from inclinometers 4, 6 and 8 (IN4, 6 and 8). These inclinometers were located approximately 95, 45 and 11 m from the nearest corner of the excavation box. A significant corner effect occurred on the short side of the excavation box; the maximum wall deflection of IN8 was reduced by half compared to IN4. In contrast, the wall movements of IN6 at all stages only showed a slight reduction (less than 15%) compared to the movements of IN4. In the Sukhumvit Station box, the excavation depth in Stage 4 was 21 m. Fig. 10 illustrates the maximum wall movements after the Stage 4 excavation for all eight inclinometers. It also shows that the corner effect, along both long sides (East: IN2, 5 and 7 and West: IN3, 4 and 6), was relatively small compared to that of the short sides (North: IN8 and South: IN1).

3.4. Ground surface settlements

The measured data of the surface settlement at Sukhumvit Station from the surface settlement array (SS1) are plotted in Fig. 11. The predicted settlement profiles from empirical methods

(Clough and O'Rourke, 1990; Hsieh and Ou, 1998; Ou and Hsieh, 2011) are also presented in Fig. 11. All three empirical methods exhibit similar surface settlement envelopes and they are in good agreement with the field measurements. However, one exception is that Clough and O'Rourke (1990) method cannot predict the surface settlements in the Secondary Influence Zone (SIZ). Additionally, the field surface settlements did not appear to extend far enough from the wall to enable the measurement of the surface settlements in the SIZ. As a result, the findings from further studies on surface settlements, using finite element analyses, will be compared with both the field measurements (within PIZ) and the predicted surface settlement envelope from the empirical estimation (within SIZ).

4. Finite element modelling

The 2D plane strain finite analysis approach, using PLAXIS v.9 software (PLAXIS 2D v.9, 2009), was adopted in this study. As the ratio of the length (L) to width (B) of the Sukhumvit Station box was high ($L/B=8.7$), the 3D effect along the long sides of the station (see Fig. 6) was small; thus, the 2D plane strain approach was considered appropriate. Only the right half of the station box (at the cross section of IN4 and IN5) was modelled because the station configuration was symmetric. A seven-layer soil profile (shown in Fig. 7) was adopted. Importantly, four soil models (i.e., Mohr–Column Model (MCM), Soft Soil Model (SSM), Hardening Soil Model (HSM) and Hardening Soil Model with Small-Strain Stiffness (HSS)) were used to evaluate their performances in the deep excavation modelling. All soil layers were modelled using 15-node elements. For the structural components (i.e., diaphragm walls, platform slabs, base slab, columns and piles), non-volume plate elements were used. The soil-diaphragm wall interaction was modelled by the zero-thickness interface element. The interface element stiffness values were in the range of 0.7–0.9, depending on the soil profile, to simulate the ground disturbance. The stiffness of the concrete was also reduced by 20% to take into account the possibility of cracking (Schweiger, 2009). Table 3 presents the input parameters of the structural components.

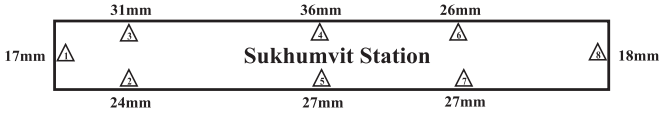

Fig. 10. Maximum horizontal movement of D-walls after stage 4 excavation.

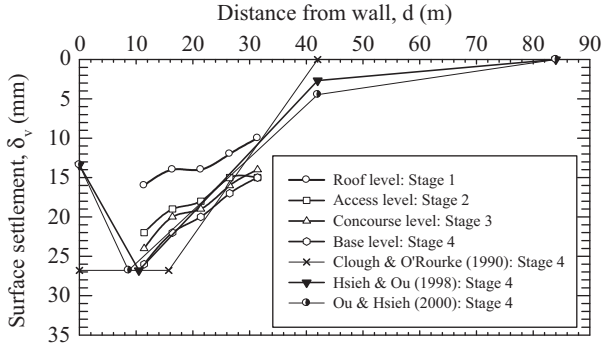

Fig. 11. Comparison between measured and predicted surface settlements.

4.1. Mesh generation

Prior to the study on the soil constitutive models, it was decided that the mesh refinement of the finite element model constructed here should be clarified. The finite element model and the mesh generation are shown in Fig. 12. The model has an average element size of 2.53 m and a total element number of 649. A finer mesh generation, with an average mesh size of 1.42 m and a total of 2054 elements, was also adopted in the study. For example, in the case of the HSM analysis, the predicted lateral wall movements and the ground surface settlements reveal almost identical wall movement profiles and surface settlement envelopes for both models. Therefore, the model with 649 elements was selected for this analysis in order to reduce the computational time.

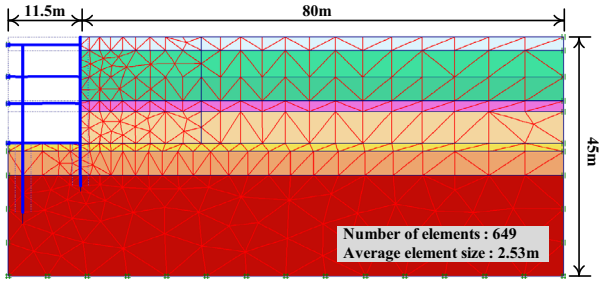

Fig. 12. Finite element model and mesh generation.

Table 3
Input parameters for structure components.

Parameter	Diaphragm wall (1 m thick)	Platform slab (1 m thick)	Base slab (1.8 m thick)	Column (0.8 m dia. at 11.4 spacing)	Pile (1.8 m dia. at 11.4 m spacing)
Axial stiffness, EA (MN/m)	28000	28000	50400	1712	3852
Flexural rigidity, EI (MN/m^2/m)	2333	2333	13608	91.3	1040
Weight, w (kN/m^2)	16.5	25	45	25	25
Poisson's ratio, ν	0.15	0.15	0.15	0.15	0.15

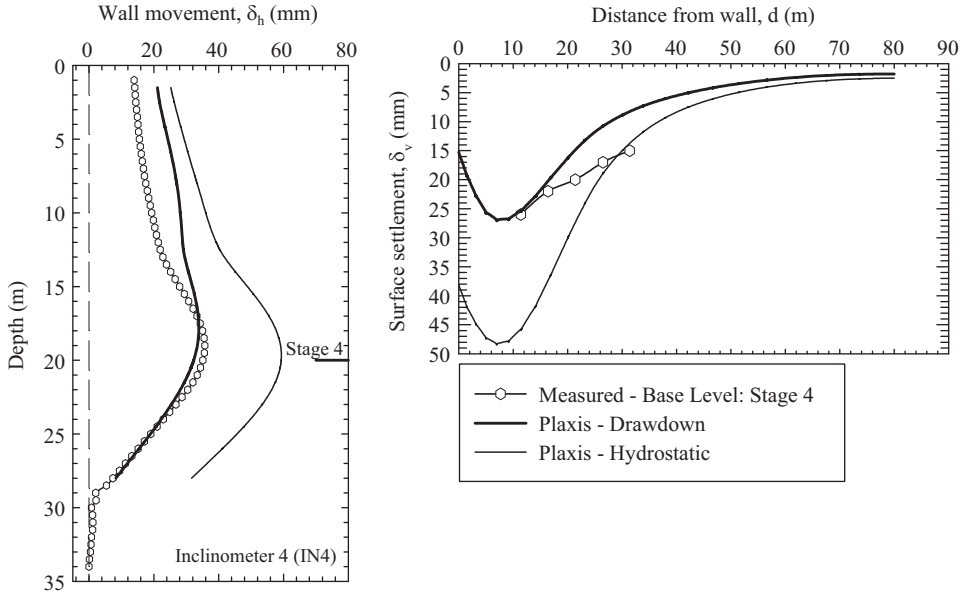

Fig. 13. Comparison of finite element predictions from drawdown and hydrostatic cases.

4.2. Effect of initial pore water pressure (hydrostatic and drawdown cases)

The pore water pressure in the Bangkok area is not hydrostatic, due to the effect of deep well pumping. Therefore, in order to investigate the effect of the initial pore water pressure condition in the finite element modelling, two analyses were conducted. The first applied a drawdown pore water pressure profile, while the second assumed a hydrostatic pore water pressure. The ground water level was set at 2.0 m below the ground surface. Fig. 3 depicts the drawdown and the hydrostatic pore water profiles. In a similar manner to the study on the mesh refinement effect, all the soil parameters, structure element parameters and the number of elements in the model were kept the same for both analyses. Only the initial pore water pressure was changed to fit the conditions described.

The results of the finite element analyses, with drawdown and hydrostatic pore water pressure conditions, are shown in Fig. 13. For both the maximum lateral wall movement and the maximum surface settlement, the hydrostatic case prediction was two times higher than the corresponding field measurements. The drawdown case seems to provide a reasonable agreement, especially for the peak values. More importantly, at the toe of the diaphragm wall, the lateral wall movement from the hydrostatic case had nearly three times the values indicated by the inclinometer. This outcome shows a high degree of instability for the diaphragm wall, which did not occur on site. It is concluded, therefore, that a realistic drawdown pore water pressure is necessary for a finite element analysis in the Bangkok area. This drawdown pore water pressure was then applied to all the analyses in the following sections.

5. Constitutive soil models and their parameters

Numerical studies on deep excavations in Bangkok subsoil are often conducted using finite element software with the Mohr–Coulomb Model. Many researchers (e.g., Teparaksa et al., 1999; Phienwej and Gan, 2003; Hooi, 2003; Phienwej, 2008; Mirjalili, 2009) have concentrated their work on back calculating the ratio of the undrained elastic modulus to the undrained shear strength (E_u/s_u). The undrained shear strength, which is determined from vane shear tests in soft clay and triaxial tests in stiffer clay, was normally adopted in the back analyses of the E_u/s_u ratio. The back analysis results of the E_u/s_u values for Bangkok subsoils are summarised in Table 4.

5.1. Soft Soil Model and Hardening Soil Model

The Soft Soil Model (SSM) has been developed within the Critical State Soil Mechanics (CSSM) framework, which is similar to Cam-Clay types of soil models.

The SSM utilises the elliptic yield surface identical to that of the Modified Cam-Clay model. However, the Mohr–Coulomb failure criterion is also adopted in the SSM to define the failure line. The seven parameters for SSM are required as input in PLAXIS, as summarised in Table 5. More details on the Soft Soil Model can be found in Brinkgreve (2002).

The Hardening Soil Model (HSM) was developed under the framework of the theory of plasticity. The total strains are calculated using a stress-dependent stiffness, in which the stiffness is different for the loading and unloading/reloading parts. The strain hardening is assumed to be isotropic, depending on plastic shear and volumetric strain. A non-associated flow rule is adopted for the frictional hardening, while an associated flow rule is assumed for the cap hardening. A total of ten input parameters are required for the HSM, as tabulated in Table 5. Schanz et al. (1999) explained in detail the formulation and the verification of the HSM.

The Soft Soil Model (SSM) was actually modified from the Modified Cam-Clay (MCC) model. The two main modifications were the use of the Mohr–Coulomb failure criterion and an

Table 4
E_u/s_u ratios resulting from finite element back analyses of previous studies.

Bangkok soil layers	E_u/s_u ratio			
	Teparaksa et al. (1999)	Phienwej and Gan (2003)	Phienwej (2008)	Mirjalili (2009)
Soft clay	500	500	500	500
Medium clay	–	700	–	500
Stiff clay	2000	1200	1200	500
Hard clay	–	–	–	1000

Table 5
Soil models input parameters.

Input parameters for			Parameters	Description	Parameter evaluation
Soft Soil Model (SSM)	Hardening Soil Model (HSM)	Hardening Soil Model with Small Strain Stiffness (HSS)			
✓	✓	✓	ϕ'	Internal friction angle	Slope of failure line from Mohr–Coulomb failure criterion
✓	✓	✓	c'	Cohesion	y-intercept of failure line from Mohr–Coulomb failure criterion
	✓	✓	R_f	Failure ratio	$(\sigma_1-\sigma_3)_f/(\sigma_1-\sigma_3)_{ult}$
✓	✓	✓	ψ	Dilatancy angle	Ratio of $d\varepsilon_v^p$ and $d\varepsilon_s^p$
✓			λ^*	Modified compression index	Slope of primary loading curve ln p' versus ε_v space
✓			κ^*	Modified swelling index	Slope of unloading/reloading curve ln p' versus ε_v space
	✓	✓	E_{50}^{ref}	Reference secant stiffness from drained triaxial test	y-intercept in $\log(\sigma_3/p^{ref})-\log(E_{50})$ curve
	✓	✓	E_{oed}^{ref}	Reference tangent stiffness for oedometer primary loading	y-intercept in $\log(\sigma_1/p^{ref})-\log(E_{oed})$ curve
	✓	✓	E_{ur}^{ref}	Reference unloading/reloading stiffness	y-intercept in $\log(\sigma_3/p^{ref})-\log(E_{ur})$ curve
	✓	✓	m	Exponential power	Slope of trend-line in $\log(\sigma_3/p^{ref})$-$\log(E_{50})$ curve
✓	✓	✓	ν_{ur}	Unloading/reloading Poisson's ratio	0.2 (default setting)
✓	✓	✓	K_0^{nc}	Coefficient of earth pressure at rest (NC state)	$1-\sin\phi'$ (default setting)
		✓	$G_{\max}^{ref}$	Reference small strain shear modulus	$G_{\max}=G_{\max}^{ref}\left(\frac{\sigma'_3+c'\cot\varphi'}{p^{ref}+c'\cot\varphi'}\right)^m$
		✓	$\gamma_{0.7}$	Shear strain amplitude at $0.722G_{\max}$	Modulus degradation curve (plot between $G/G_{\max}$and log γ)

Remarks: σ_1 is major principal stress (kN/m^2).
σ_3 is minor principal stress (kN/m^2).
p^{ref} is reference pressure (100 kN/m^2).

improvement in the volumetric yield surface. Parameters λ^* and κ^*, as used in the MCC, remain the same in the SSM. Two additional parameters, namely, ν_{ur} and K_o^{nc}, were introduced. The influence of both parameters on the triaxial (q versus ε_a and q versus p') behaviour and the oedometer (ε_v versus log p') behaviour, resulting from the parametric study, has been discussed in Surarak et al. (2012). Table 6 presents the parameters from the SSM analysis for the BSC, MC, 1st SC, 2nd SC and HC layers. The HSM was applied to the MG and CS layers instead of the SSM. The critical state soil model, which forms the basis of the MCC and SSM models, was developed especially to simulate soft clay behaviour. Therefore, the SSM is not suitable for the MG or CS layers. Also, soil movements owing to the excavation of the MG and CS layers are relatively small compared to the BSC, 1st SC and 2nd SC layers. Consequently, using the HSM instead of the SSM in the MG and CS layers will have a negligible influence on this analysis. Parameters λ^* and κ^* were obtained from the consolidation characteristics of Bangkok clays. Hence, ν_{ur} and K_o^{nc} are set according to the results of the parametric studies. Table 7 presents the parameters from the HSM analysis for the MG, BSC, MC, 1st SC, CS, 2nd SC and HC layers. All soil layers are assumed to have no dilatancy ($\psi=0^o$). More details on the parametric studies of Bangkok clays can be seen in Surarak et al. (2012).

Table 6
Parameters for Soft Soil Model (SSM) analysis.

Layer	Soil type	Depth (m)	λ^*	κ^*	ν_{ur}	K_o^{nc}
1	MG	0–2.5	HSM			
2	BSC	2.5–12	0.12	0.02	0.2	0.7
3	MC	12–14	0.1	0.009	0.2	0.6
4	1st SC	14–20	0.045	0.009	0.2	0.5
5	CS	20–21.5	HSM			
6	2nd SC	21.5–26	0.045	0.009	0.2	0.5
7	HC	26–45	0.006	0.0009	0.2	0.5

Remarks:

1. The strength parameters (ϕ' and c'), dilatancy angle (ψ) and bulk unit weight for the SSM analysis are the same as those for the HSM analysis (Table 7).
2. HSM is adopted for the Made Ground (MG) and Clayey Sand (CS) layers.

5.2. Hardening Soil Model with Small Strain Stiffness (HSS)

The Hardening Soil Model with Small Strain Stiffness (HSS) is a modification of the HSM, incorporating the small strain stiffness of soils (Benz, 2006). The model employs a modified hyperbolic law for the stiffness degradation curve (Hardin and Drnevich, 1972; Santos and Correia, 2001) as in the following equation:

$$\frac{G}{G_{\max}} = \frac{1}{1+a\left|\frac{\gamma}{\gamma_{0.7}}\right|} \tag{3}$$

Two additional parameters, namely, the small strain shear modulus ($G_{\max}$), where G=0.722$G_{\max}$, and the reference shear strain ($\gamma_{0.7}$), are utilised to govern the soil stiffness at a small strain level. The input parameters for the HSM, presented in Table 7, remain the same for the HSS analysis. All input parameters for the HSM are carried over to the HSS model, with the two additional parameters, $G_{\max}$ and $\gamma_{0.7}$ (see Table 5). However, knowledge of the small strain parameters for the MG, SC and HC layers is very limited. Additionally, the expected soil movements arising from these layers are small in comparison to the BSC, MC, 1st SC and 2nd SC layers. Therefore, the HSM is used in the MG, CS and HC layers. The HSS is only applied to the predominant layers, i.e., BSC, MC, 1st SC and 2nd SC.

Detailed studies of small strain parameters $G_{\max}$ and $\gamma_{0.7}$ of the Bangkok clays were studied by Likitlersuang, et al., (2013). The shear modulus at a small strain ($G_{\max}$) was obtained from both the in situ tests (down-hole and seismic cone tests) and the laboratory tests using bender elements. Hence, parameter $G_{\max}$ is considered to be reliable and is selected straight from the test results, as listed in Table 8. Parameter $\gamma_{0.7}$ is, on the other hand, considered to have more variation. The two empirically based methods (Ishibashi and Zhang, 1993; Vucetic and Dobry, 1991) are used to calculate the $\gamma_{0.7}$ of the Bangkok clays, as shown in Fig. 14. Both methods estimated similar results for the Bangkok Soft Clay layer, which also coincide with the results of the bender element tests on the Bangkok soft clay (Teachavorasinskun et al., 2002). The two sets of Hardening Soil Models with Small Strain Stiffness analyses (HSS 1 and HSS 2) are considered herein. For the HSS 1 analysis, the average values of $\gamma_{0.7}$ for the BSC and MC layers from both methods, namely, Ishibashi and Zhang (1993) and Vucetic and Dobry (1991), are used (see Fig. 14). Details on the small strain stiffness parameters for Bangkok clays can be found in Likitlersuang, et al., (2013).

5.3. Mohr–Coulomb model (MCM)

The concept of the total stress analysis (ϕ=0) with the Mohr–Coulomb Model (MCM) for clayey soils has been widely used in geotechnical engineering practice. One of the major advantages of this concept is that the soil parameters are easy to obtain, as only undrained shear strength (s_u) and undrained elastic modulus (E_u) are needed for the rapid loading conditions. The undrained shear strength of the Bangkok subsoils, obtained from the vane shear and triaxial tests, will be used to govern the strength of the Bangkok Soft Clay (BSC), Medium Clay (MC), 1st Stiff Clay (1st SC), 2nd Stiff Clay (2nd SC) and Hard Clay (HC). Back analyses of the deep excavation problems in Bangkok subsoils (Teparaksa et al., 1999; Phienwej and Gan, 2003) have shown that the E_u/s_u ratios of 500 and 1000–2000 give a reasonable agreement between the measured and the predicted wall movements. In the current study, a E_u/s_u of 500 was adopted in the BSC, MC and 1st SC layers. Higher values of E_u/s_u=600 and 1000 were used for the 2nd SC and HC layers. These values for E_u/s_u were selected based on the previous studies, as summarised in Table 4. The MG and CS layers were modelled using drained analyses. The drained moduli were estimated from the SPT N values from the adjacent boreholes. Table 9 summarises all the parameters used in the MCM analysis.

5.4. Calibrations of soil parameters

The stiffness and strength parameters for the SSM and HSM of soft and stiff Bangkok clays have been numerically studied

Table 7
Parameters for Hardening Soil Model (HSM) analysis.

Layer	Soil type	Depth (m)	γ_b (kN/m^3)	c' (kPa)	ϕ' (^{o})	ψ(^{o})	E_{50}^{ref} (MPa)	E_{oed}^{ref} (MPa)	E_{ur}^{ref}(MPa)	ν_{ur}	m	K_o^{nc}	R_f	Analysis type
1	MG	0–2.5	18	1	25	0	45.6	45.6	136.8	0.2	1	0.58	0.9	Drained
2	BSC	2.5–12	16.5	1	23	0	0.8	0.85	8.0	0.2	1	0.7	0.9	Undrained
3	MC	12–14	17.5	10	25	0	1.65	1.65	5.4	0.2	1	0.6	0.9	Undrained
4	1st SC	14–20	19.5	25	26	0	8.5	9.0	30.0	0.2	1	0.5	0.9	Undrained
5	CS	20–21.5	19	1	27	0	38.0	38.0	115.0	0.2	0.5	0.55	0.9	Drained
6	2nd SC	21.5–26	20	25	26	0	8.5	9.0	30.0	0.2	1	0.5	0.9	Undrained
7	HC	26–45	20	40	24	0	30.0	30.0	120.0	0.2	1	0.5	0.9	Undrained

Table 8
Parameters for Hardening Soil Model with Small Strain Stiffness (HSS 1 and 2).analyses.

Layer	Soil type	Depth (m)	G_{max} (MPa)	$\gamma_{0.7}$ (%) for HSS 1	$\gamma_{0.7}$ (%) for HSS 2
1	MG	0–2.5		HSM	
2a	BSC 1	2.5–7.5	7	0.056	0.056
2b	BSC 2	7.5–12	10	0.08	0.08
3	MC	12–14	12	0.09	0.09
4	1st SC	14–20	30	0.1	0.002
5	CS	20–21.5		HSM	
6	2nd SC	21.5–26	50	0.1	0.002
7	HC	26–45		HSM	

Remarks:

1. The strength parameters (ϕ' and c'), dilatancy angle (ψ) and bulk unit weight for the SSM analysis are the same as those for the HSM analysis (Table 7).
2. HSM is adopted for the Made Ground (MG), Clayey Sand (CS) and Hard Clay (HC) layers.

using PLAXIS finite element software (Surarak et al., 2012; Likitlersuang et al., 2013). The numerical study was based on a comprehensive set of experimental data on Bangkok subsoils from oedometer and triaxial tests carried out at the Asian Institute of Technology as well as the cyclic triaxial tests carried out at Chulalongkorn University. The determined HSM parameters are the Mohr–Coulomb effective stress strength parameters together with the stiffness parameters, namely, tangent stiffness for primary oedometer loading, secant stiffness in undrained and drained triaxial tests, unloading/reloading stiffness and the power for stress-level dependency of stiffness. Details can be found in Surarak et al. (2012). In addition, the small strain stiffness parameters for the HSS model of Bangkok clays were recently published in Likitlersuang et al. (2013).

6. Finite element analysis result for Sukhumvit Station

A finite element analysis of the Sukhumvit Station excavation is studied in this section. Due to symmetrical geometry, one half of the station was modelled (as shown in Fig. 12). The calculation steps followed the construction sequences, as tabulated in Table 2. The four stages of the FEM results, where the excavation depths were at 1.5, 7.5, 12.5 and 21 m (Fig. 8), were compared with the monitoring data. Note that all the measured data were recorded within one week after the excavation reached the desired levels in order to retain the undrained condition.

6.1. Results and discussions on FEA with Mohr–Coulomb model (MCM)

Fig. 15 shows the measured and predicted lateral wall movements and ground surface settlements for the Sukhumvit Station box excavation using MCM. The ground surface settlement predicted by Hsieh and Ou (1998) at the Stage 4 excavation was also included for comparison. The predictions given by the MCM analysis slightly underpredict the lateral wall movements at all stages of the excavation. The maximum lateral movement of the wall at the final excavation stage is about 15% lower that the measured value. Contrary to the lateral movement, the MCM analysis shows a much shallower and wider surface settlement profile, when compared to the field measurement and empirical prediction. The predicted maximum surface settlement at the final excavation stage was less than one half of the field measurement. Similar trends in surface settlement profiles of the MCM prediction of surface settlements can be found in the literature (Kung et al., 2009; Schweiger, 2009).

It should be pointed out that wider settlement envelopes, as predicted by the MCM, lead to the overprediction of the surface settlements in the Secondary Influence Zone (SIZ). Nevertheless, a flatter settlement envelope is expected to lead

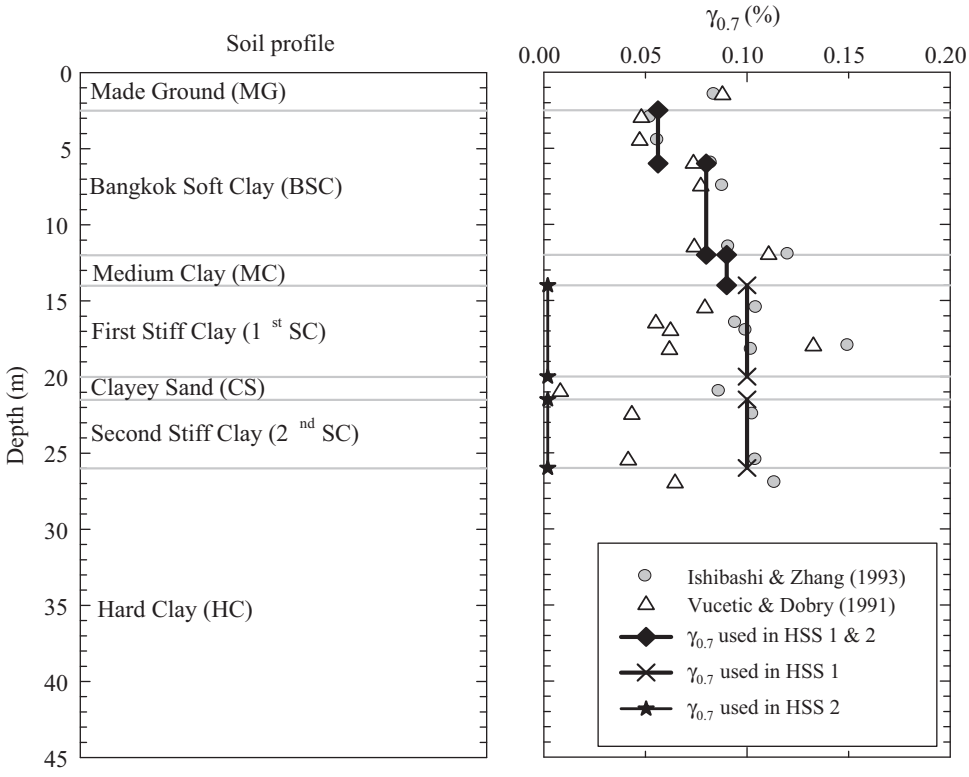

Fig. 14. Parameter $\gamma_{0.7}$ as used in HSS 1 and HSS 2 models.

Table 9
Parameters for Mohr–Coulomb Model (MCM) analysis.

Layer	Soil type	Depth (m)	γ_b (kN/m^3)	s_u (kPa)	c' (kPa)	ϕ' (^{o})	ψ (^{o})	E_u (MPa)	E' (MPa)	ν	Analysis type
1	MG	0–2.5	18	–	1	25	0	–	8	0.3	Drained
2a	BSC 1	2.5–7.5	16.5	20	–	–	0	10	–	0.495	Undrained
2b	BSC 2	7.5–12	16.5	39	–	–	0	20.5	–	0.495	Undrained
3	MC	12–14	17.5	55	–	–	0	27.5	–	0.495	Undrained
4	1st SC	14–20	19.5	80	–	–	0	40	–	0.495	Undrained
5	CS	20–21.5	19	–	1	27	0	–	53	0.25	Drained
6	2nd SC	21.5–26	20	120	–	–	0	72	–	0.495	Undrained
7	HC	26–45	20	240	–	–	0	240	–	0.495	Undrained

to less predicted differential settlements for the buildings located at the transition of the PIZ and SIZ.

6.2. Results and discussions on FEA with Soft Soil Model (SSM)

The predicted lateral wall movement profiles and surface settlement envelopes were predicted from the SSM analysis are shown in Fig. 16. Furthermore, these predicted lateral wall movements at Stages 1–3 are fairly close to the field measurements. The maximum lateral wall movement at the final stage slightly underpredicted the measured values by approximately 15% (similar to MCM predictions). In terms of the ground surface settlement predictions, the SSM gave better trends for the settlement envelope compared to the MCM. Nevertheless, the same general trend of shallower and wider settlement envelopes was observed.

6.3. Results and discussions on FEA with Hardening Soil Model (HSM)

The strength and stiffness parameters from the study by Surarak et al. (2012) are used as inputs for the HSM analysis in this section. The input parameters listed in Table 7 are the results of the parametric studies and the undrained triaxial test series back-calculations. More specifically, the following procedure was adopted:

(a) The E_{50}^{ref} used in the analyses of the drained materials (MG and CS) was estimated from the SPT N values for

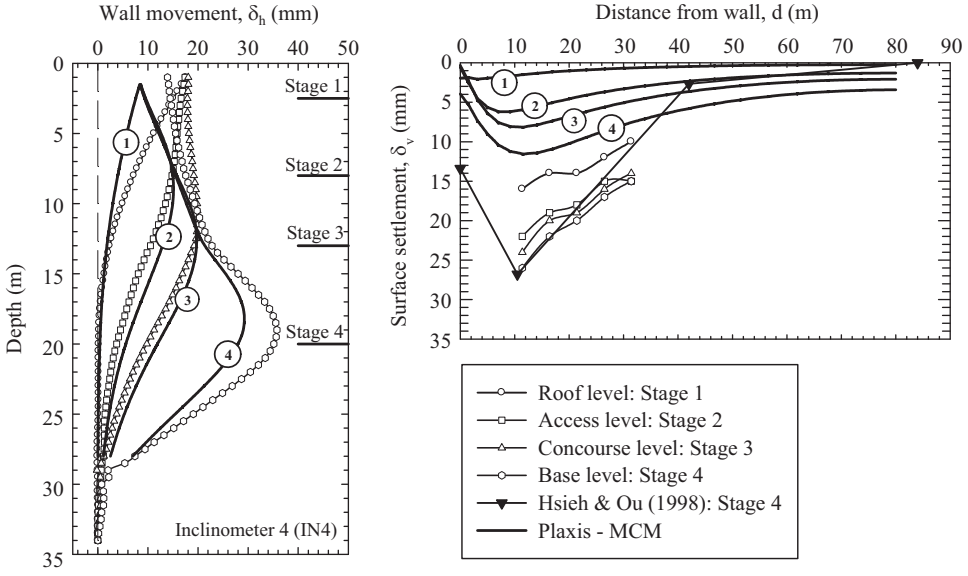

Fig. 15. Measured and predicted lateral wall movements and surface settlements from MCM analysis.

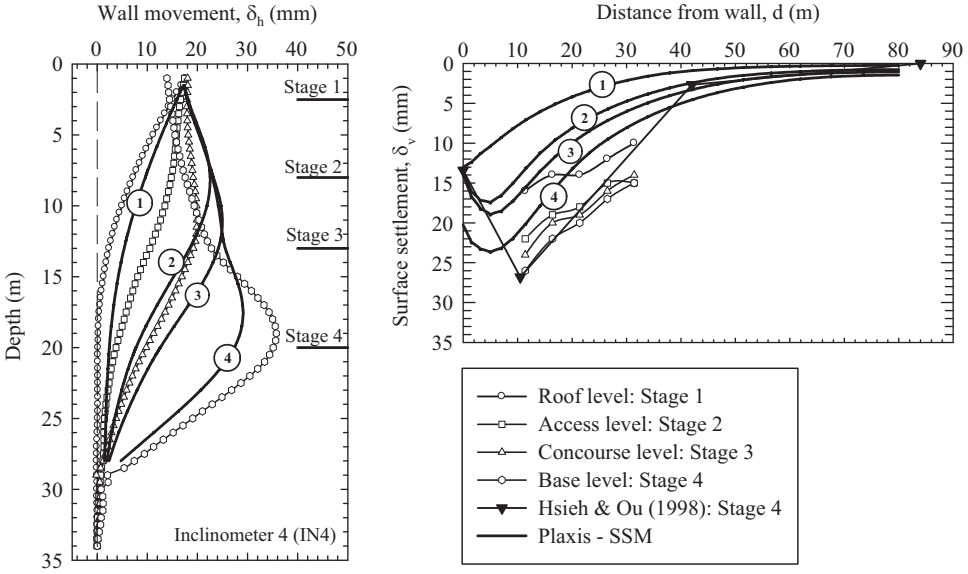

Fig. 16. Measured and predicted lateral wall movements and surface settlements from SSM analysis.

the adjacent boreholes. The ratios of $E_{oed}^{ref} = E_{50}^{ref}$ and $E_{ur}^{ref} = 3E_{50}^{ref}$ were suggested by Brinkgreve (2002).

(b) For BSC, MC, 1st SC, 2nd SC and HC, the procedure for the triaxial and oedometer modelling was adopted. The triaxial and oedometer test results from samples taken from the adjacent boreholes were used in the stiffness moduli back-calculation.

(c) Parameters ν_{ur}, m and R_f were kept as 0.2, 1 and 0.9, respectively. These values were suggested in Surarak et al. (2012).

Fig. 17 compares the measured lateral wall movements and the ground surface settlements with those predicted by the HSM. The predicted lateral wall movements at all excavation stages within the BSC layer (depths of 2.5–12 m) were slightly higher than the field measurements. This overestimation extends further into the deeper layers for excavation Stages 1–3. The maximum lateral movement in the last excavation stage (located in the 1st and 2nd SC layers) agrees well with the measured values. In the case of the ground surface settlement comparison, the HSM predicted better settlement envelopes than MCM or SSM. However, the settlements within the SIZ were still slightly larger than the predictions using the Hsieh and Ou (1998) method.

6.4. Results and discussions on FEA using Hardening Soil Model with Small Strain Stiffness (HSS)

The results from the HSS 1 analysis are shown in Fig. 18. The HSS 1 analysis improved the lateral wall movement prediction,

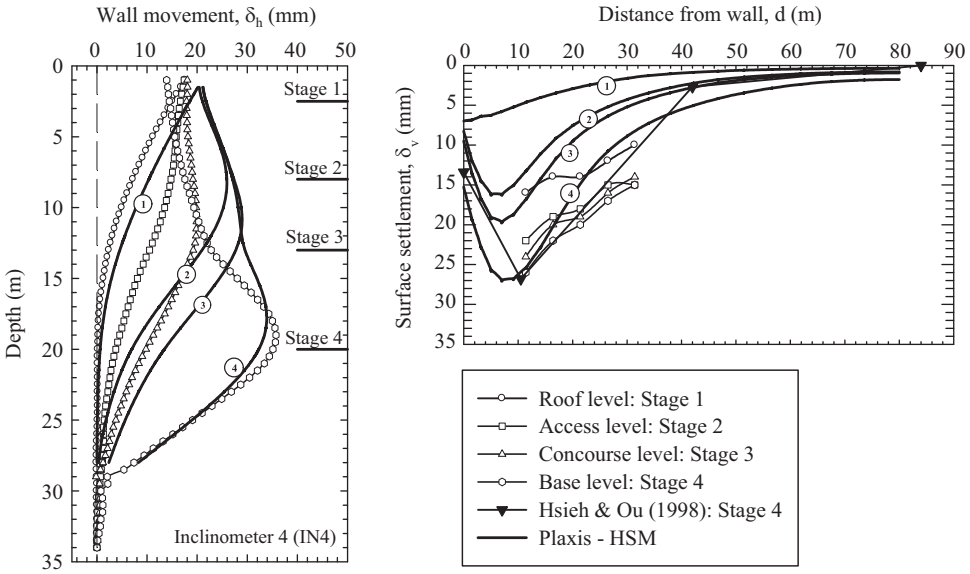

Fig. 17. Measured and predicted lateral wall movements and surface settlements from HSM analysis.

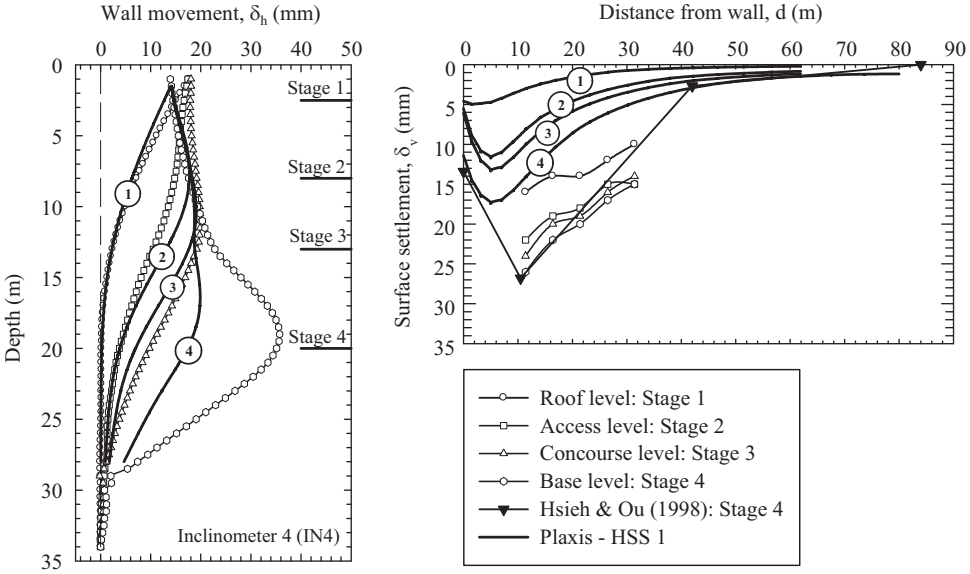

Fig. 18. Measured and predicted lateral wall movements and surface settlements from HSS 1 analysis.

when compared to those predicted by the HSM for all excavation stages in the BSC and MC layers. However, the predictions for the deeper layers (1st SC, CS and 2nd SC) were much smaller than in the HSM analysis. Indeed, the predicted maximum lateral wall movement was only one half of the measured magnitude. The corresponding surface settlements were also underpredicted by the HSS 1 analysis. This outcome confirmed that the parameters ($\gamma_{0.7}$) calculated by the Ishibashi and Zhang (1993) and the Vucetic and Dobry (1991) methods for the BSC and MC layers are valid. This conclusion was not true, however, for the Stiff Clay layers. However, there is no information on the laboratory $\gamma_{0.7}$ available for Bangkok Stiff Clay. It is suggested that a more refined analysis would be appropriate before any definite conclusion can be made on the values for the small strain stiffness of Bangkok Stiff Clay, especially when a better set of laboratory and field data is available. For the purpose of this study, it was decided that a back-fitted value of $\gamma_{0.7}$ should be adopted.

In the second HSS analysis (HSS 2), only parameter $\gamma_{0.7}$ in 1st SC and 2nd SC was adjusted to obtain the best fit results. The best fit value of $\gamma_{0.7}$ for both layers was obtained as 0.002% (see also Table 8 and Fig. 19). The predictions of the wall movements and the surface settlements, obtained by the HSS 2 analysis, are depicted in Fig. 19. As far as the results in the final stage are concerned, both the predicted lateral wall movements and the surface settlements agree well with the measured data.

7. Comparisons of FEM results

In this section, the results from the MCM, SSM, HSM and HSS 2 analyses are compared according to the stage construction.

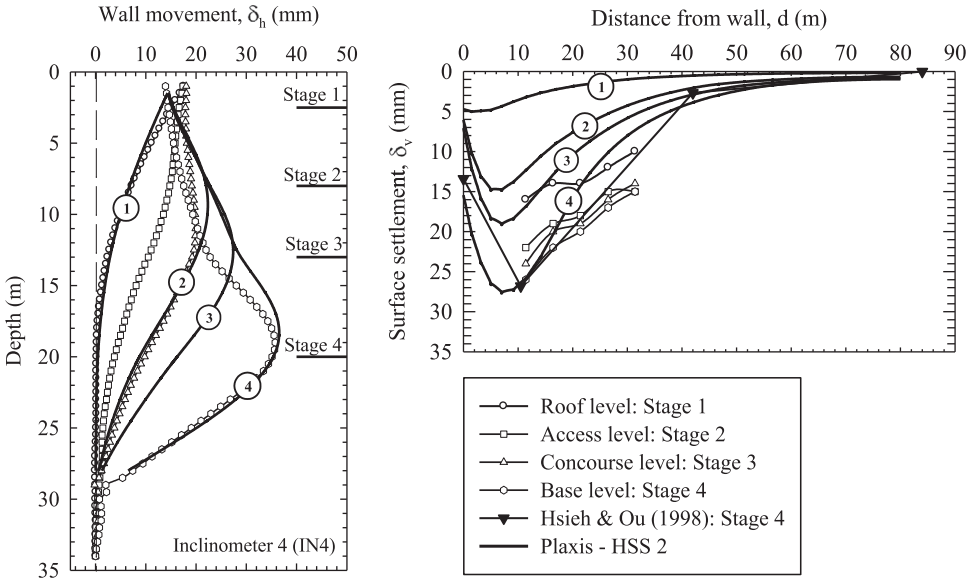

Fig. 19. Measured and predicted lateral wall movements and surface settlements from HSS 2 analysis.

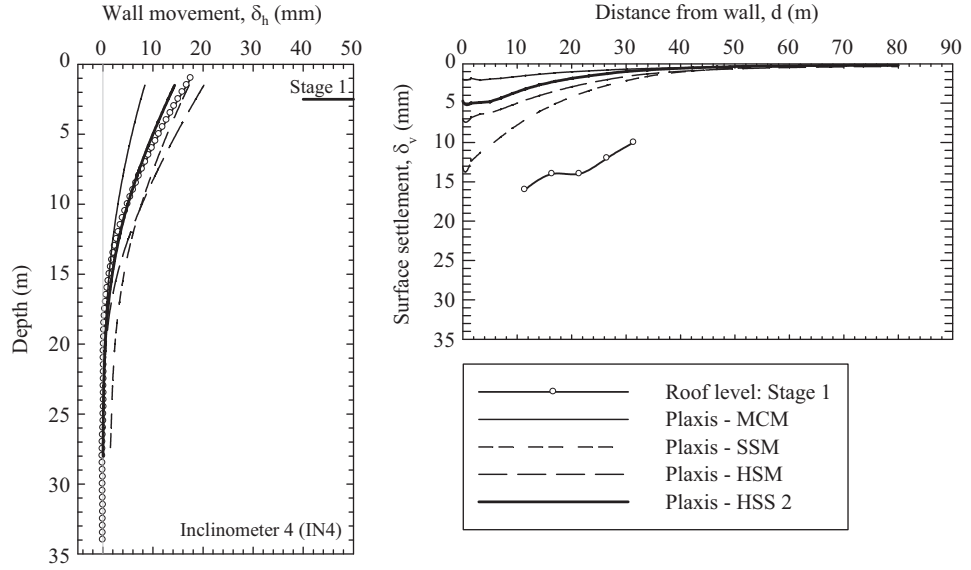

Fig. 20. Measured and predicted lateral wall movements and surface settlements at Stage 1 from MCM, SSM, HSM and HSS 2 analyses.

Figs. 20–23 show the measured and the predicted lateral wall movements and surface settlements arising from Stages 1 to 4 of the excavation, respectively. As far as the wall movements after the first stage construction are concerned, the SSM, HSM and HSS 2 provide reasonably good predictions compared to the measured data, while the MCM give a slightly underpredicted movement. The surface settlement profiles from all four analyses are smaller than the field measurements. The maximum surface settlements from the largest to the smallest are in the following order: the SSM, HSM, HSS 2 and MCM. The same trend is seen for the predicted wall movements and the ground surface settlements from the Stages 2 and 3 analyses. The predicted wall movements from the SSM, HSM and HSS 2 analyses had very similar magnitudes. Their predictions agree with the measurements at the top part of the D-wall, but slightly over-predicted the wall movements from the depth of excavation to the lower end of the D-wall. The MCM prediction, on the other hand, matches well with the measurements at the depth of excavation. However, the MCM analysis yields a smaller prediction at the top part of the D-wall. The predicted surface settlements at Stages 2 and 3 from the SSM, HSM and HSS 2 analyses are nearly identical. The shapes of their predicted settlement profiles are much steeper than that of the MCM analysis. For Stage 4 of the excavation, all four models produce generally good predictions of the wall movements. However, the HSS 2 analysis shows the best prediction of the maximum wall movement compared to the field data. For the surface settlements, the HSM and HSS 2 show nearly identical settlement profiles. Their results, at the final stage,

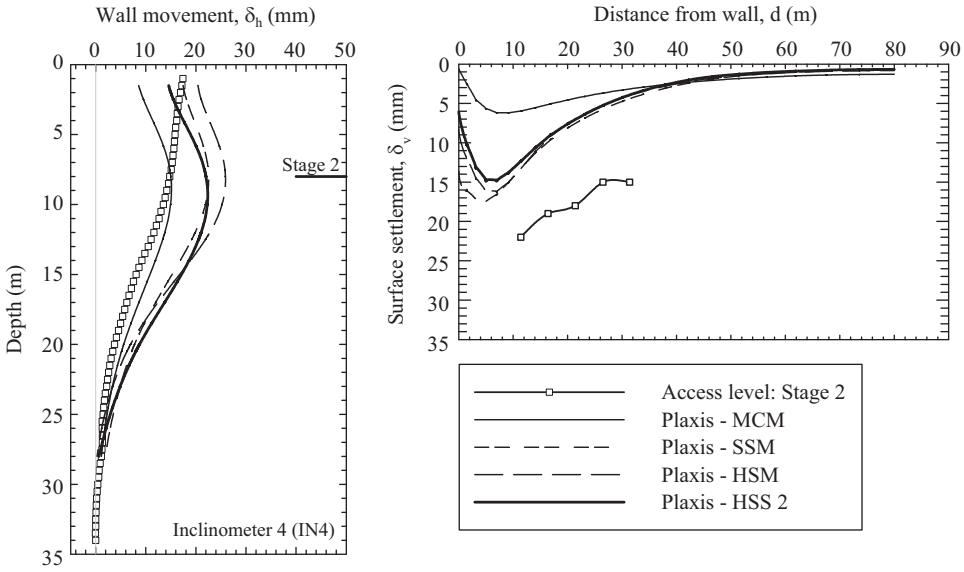

Fig. 21. Measured and predicted lateral wall movements and surface settlements at Stage 2 from MCM, SSM, HSM and HSS 2 analyses.

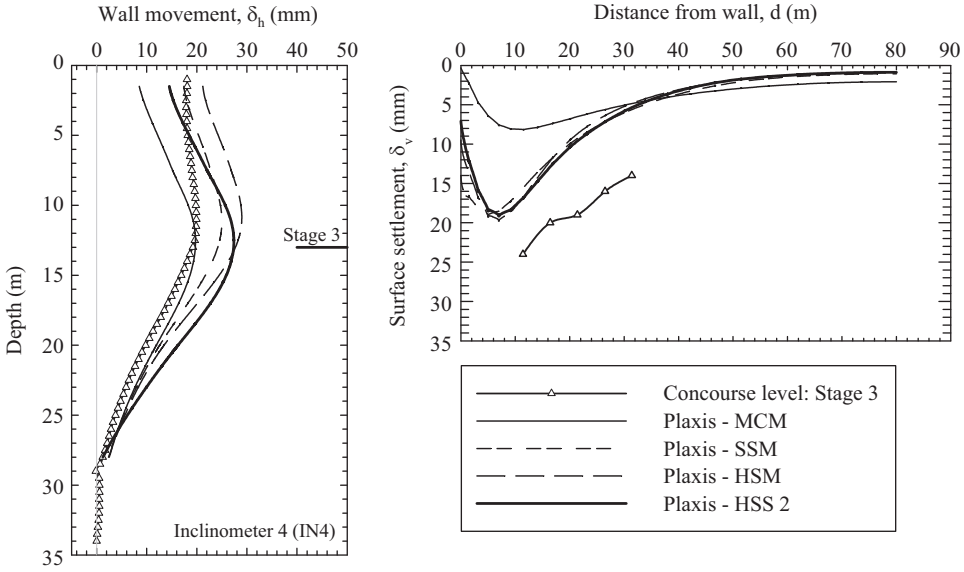

Fig. 22. Measured and predicted lateral wall movements and surface settlements at Stage 3 from MCM, SSM, HSM and HSS 2 analyses.

also agree with the field data. The MCM's settlement profile is much shallower and wider than the measured surface settlement. Its maximum surface settlement is lesser than half of the measured data. The settlement prediction from the SSM lies in between the results of the MCM and HSM analyses.

8. Concluding remarks

This paper investigates the behaviour of D-wall movements and ground surface settlements by means of empirical and numerical analyses. An underground station excavation of the Bangkok MRT Blue Line project was used as a case study. Based on the results of the study, the most important points are summarised as follows.

(1) Inclinometer measurements from Sukhumvit Station showed that the 3D effects on the long sides of the D-wall are small compared to the effects on the short sides. This evidence confirmed other studies on the 3D effects of deep excavations (Ou et al., 1993).
(2) The predicted surface settlement profiles coincided with the observed data within the Primary Influence Zone. However, the ground surface settlement measurements did not extend far enough to make a comparison in the Secondary Influence Zone.
(3) Considerable differences were found from the FEM analyses with hydrostatic and drawdown pore water conditions. The case of more realistic drawdown pore pressure predicted closer lateral wall movements and ground surface settlements compared to field observations.

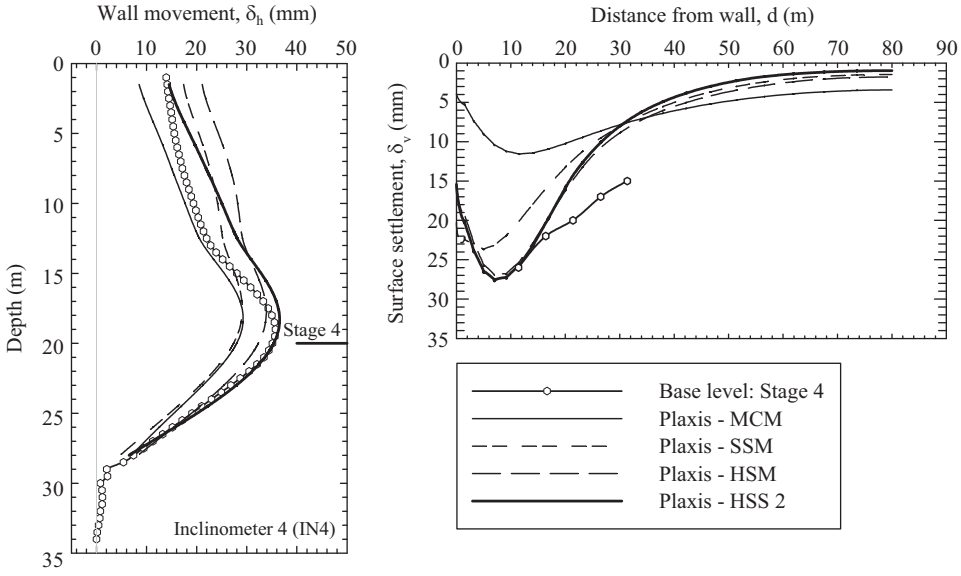

Fig. 23. Measured and predicted lateral wall movements and surface settlements at Stage 4 from MCM, SSM, HSM and HSS 2 analyses.

(4) In general, better lateral wall movements and ground surface settlements were obtained from higher degrees of sophistication of constitutive models in the following order, i.e., MCM, SSM, HSM and HSS. Nonetheless, no salient differences between the results of axial force, shear force and bending moment predictions were observed.
(5) Back-calculated E_u/s_u ratios from the literature can be used reasonably well for lateral movement predictions with MCM. However, accurate ground surface settlements were not obtained.
(6) SSM and HSM analyses with soil parameters interpreted from laboratory and in situ tests (Surarak et al., 2012), provided better agreement with lateral wall movements and surface settlement field observations.
(7) Results from the HSS analysis confirmed the values of $\gamma_{0.7}$ in BSC, as predicted by Ishibashi and Zhang (1993) and Vucetic and Dobry (1991). In the case of the Stiff Clay, however, a back-calculated $\gamma_{0.7}$ of 0.002% is necessary for better lateral wall movements and surface settlement predictions.
(8) As a consequence of this study, it can be stated that no matter what analysis or numerical method is employed, a good prediction of the ground movements cannot be achieved unless relevant parameters are selected. In the case of FEM, a suitable simulation process also needs to be adopted.

Acknowledgements

The authors wish to thank the late president of the Mass Rapid Transit Authority of Thailand (MRTA), Mr. Chukiat Phota-yanuvat, and the MRTA engineers for their kindness in encouraging us and providing relevant data for carrying out the academic research activities related to this important work. The first author would also like to extend his appreciation for the research funding from the Stimulus Package 2 (SP2) of the Ministry of Education, Thailand under the theme of Green Engineering for Green Society. The second author would like to thank Professor Suchatvee Suwansawat, of the King Mongkut's Institute of Technology, Ladkrabang, Thailand, for his kind assistance during the data collection.

References

Benz, T., 2006. Small-Strain Stiffness of Soils and its Numerical Consequences. Doctoral Thesis, Institute of Geotechnical Engineering, University of Stuttgart, Stuttgart.
Bourgeois, E., Kouby, A.L., Soyez, L., 2012. Influence of the strip-backfill interaction model in the analysis of the behavior of a mechanical stabilized earth wall. Soils and Foundations 52 (3), 550–561.
Brinkgreve, R.B.L., 2002. Plaxis 2D – version 8 manuals. A.A. Balkema, Netherlands.
Clough, G.W., O'Rourke, T.D., 1990. Construction-Induced Movements of In situ Walls, Design and Performance of Earth Retaining Structure. 2. ASCE Special Publication 439–470.
Hardin, B.O., Drnevich, V.P., 1972. Shear modulus and damping in soils: design equations and curves. Journal of Soil Mechanics and Foundations Division, 98; 667–692.
Hooi, Y.K., 2003. Ground Movements Associated with Station Excavation of the First Bangkok MRT subway. Masters Thesis, Asian Institute of Technology, Thailand.
Hsieh, P.G., Ou, C.Y., 1998. Shape of ground surface settlement profiles caused by excavation. Canadian Geotechnical Journal 35 (6), 1004–1017.
Ishibashi, I., Zhang, X., 1993. Unified dynamic shear moduli and damping ratios of sand and clay. Soils and Foundations 33 (1), 182–191.
Kempfert, H., Gebreselassie, B., 2006. Excavations and Foundations in Soft Soils. Springer-Verlag, Berlin, Heidelberg, Germany.
Kung, G.T., Ou, C.Y., Juang, C.H., 2009. Modelling small-strain behaviour of Taipei clays for finite element analysis of braced excavations. Computer and Geotechnics 36 (1–2), 304–319.
Likitlersuang, S., Teachavorasinskun, S., Surarak, C., Oh, E., Balasubramaniam, A.S., 2013. Small Strain Stiffness and Stiffness Degradation Curve of Bangkok Clays. Soils and Foundations 53 (4), 498–509.

Mirjalili, R., 2009. Performance of Deep Excavations in MRT Stations: Bangkok MRT as a Case Study. Masters Thesis, Griffith University, Australia.

Ou, C.Y., 2006. Deep excavation: Theory and Practice. Taylor & Francis, London, UK.

Ou, C.Y., Hsieh, P.G., 2011. A simplified method for predicting ground settlement profiles induced by excavation in soft clay. Computers and Geotechnics 38 (12), 987–997.

Ou, C.Y., Hsieh, P.G., Chiou, D.C., 1993. Characteristics of ground surface settlement during excavation. Canadian Geotechnical Journal 30, 758–767.

Peck, R.B., 1969. Deep excavations and tunnelling in soft ground. In: Proceeding of the 7th International Conference on Soil Mechanics and Foundations Engineering. Mexico City, State of the Art Volume, pp. 225–290.

Phienwej, N., 2008. Ground movement in station excavations of Bangkok first MRT. In: Proceedings of the 6th International Symposium on Tunnelling for Urban Development (IS-Shanghai 2008), Shanghai, China, pp. 181–186.

Phienwej, N., Gan, C.H., 2003. Characteristics of ground movement in deep excavations with concrete diaphragm walls in Bangkok soils and their prediction. Journal of the Southeast Asian Geotechnical Society 34 (3), 167–175.

PLAXIS 2D v.9, 2009, Reference Manual.

Santos, J.A., Correia, A.G., 2001. Reference threshold shear strain of soil: its application to obtain a unique strain-dependent shear modulus curve for soil. In: Proceedings of the 15th International Conference on Soil Mechanics and Geotechnical Engineering, vol. 1, Istanbul, A.A. Balkema, pp. 267–270.

Schanz, T., Vermeer, P.A., Bonnier, P.G., 1999. The Hardening Soil Model: Formulation and Verification. Beyond 2000 in Computational Geotechnics. Taylor & Francis, Rotterdam.

Schweiger, H.F., 2009. Influence of constitutive model and EC7 design approach in FEM analysis of deep excavations. In: Proceeding of ISSMGE International Seminar on Deep Excavations and Retaining Structures, Budapest, pp. 99–114.

Surarak, C., Likitlersuang, S., Wanatowski, D., Balasubramaniam, A., Oh, E., Guan, H., 2012. Stiffness and strength parameters for hardening soil model of soft and stiff Bangkok clays. Soils and Foundations 52 (4), 682–697.

Suwansawat, S., 2002. Earth Pressure Balance (EPB) Shield Tunnelling in Bangkok: Ground Response and Prediction of Surface Settlements Using Artificial Neural Networks. Doctoral Thesis, Massachusetts Institute of Technology, USA.

Suwansawat, S., Chaiwonglek, C., Horny, U., 2007. Design aspects of NATM and cut and cover underground stations for the Bangkok MRTA Blue Line Extension. In: Proceedings of the 7th International Symposium on Tunnelling for Urban Development (IS-Pattaya 2007), Pattaya City, Thailand, pp. 64–75.

Teachavorasinskun, S., Thongchim, P., Lukkunaprasit, P., 2002. Shear modulus and damping of soft Bangkok clays. Canadian Geotechnical Journal 39 (5), 1201–1208.

Teparaksa, W., Thasananipan, N., Tanseng, P., 1999. Analysis of lateral wall movement for deep braced excavation of bangkok subsoils. In: Proceeding of the Civil and Environmental Engineering Conference, Bangkok, Thailand, pp. 67–76.

Vucetic, M., Dobry, R., 1991. Effect of soil plasticity on cyclic response. Journal of Geotechnical Engineering 117 (1), 89–107.